羌塘中生代盆地大洋缺氧事件及全球对比

付修根[1,2,3],王剑[1,2,3],曾玉红[1,2],宋春彦[4],曾胜强[4]
1)西南石油大学羌塘盆地研究院,成都,610050;
2)西南石油大学地球科学与技术学院,成都,610050;
3)油气藏地质及开发工程国家重点实验室(西南石油大学),成都,610050;
4)中国地质调查局成都地质调查中心,成都,610081

内容提要:位于藏北高原的羌塘盆地保存了我国最大面积的侏罗纪海相盆地,记录了较为完整的中生代海相序列。在羌塘中生代(T_3—K_1)盆地演化过程中,发生了多次水体缺氧事件,这些缺氧事件是全球大洋缺氧事件在羌塘盆地的反映。本文对这些缺氧事件的最新研究成果进行了介绍。羌塘盆地海相T—J界线剖面的碳同位素表现为两次明显的负偏异常,对应于全球T—J典型界线剖面碳同位素的"初始负偏移"和"主要负偏移",T—J之交水体由氧化环境变为缺氧环境。在盆地演化早期,在毕洛错地区识别出早侏罗世托儿期碳同位素负偏异常,可与全球早侏罗世托尔期大洋缺氧事件的碳同位素负偏进行精确地对比,揭示了早侏罗世托儿期全球缺氧事件在羌塘盆地的普遍性。在盆地演化晚期,海水逐渐从北羌塘拗陷西北部退出盆地,广泛沉积了一套黑色页岩、油页岩、泥岩及泥灰岩的岩石组合,碳同位素特征可与南特提斯、北特提斯及西北特提斯对应时期的碳同位素相对比,是早白垩世巴雷姆期全球大洋缺氧事件在羌塘盆地的反映。

关键词:海相T—J界线(海相J/T界线);托儿期缺氧事件;巴雷姆期缺氧事件;羌塘盆地

晚三叠世末,受全球构造作用及海平面变化的影响,我国除西藏外的大部分地区开始接受陆相沉积。与海相盆地相比,陆相盆地由于小的水体面积更容易受到气候变化的影响(Fu Xiugen et al.,2015),从而导致陆相剖面岩性和岩相的横向变化大,生态复杂,动植物分化程度高,难以实现区域性和全球性对比。这也限制了我国对中生代大洋重大地质事件的理解。

位于青藏高原腹地的羌塘盆地,保存了我国最大面积的侏罗纪海相盆地,记录了较为完整的中生代海相地层(王剑等,2004),是我国研究中生代大洋重大地质事件的理想地区。晚三叠世,受古特提斯洋关闭的影响,羌塘盆地整体隆升,北羌塘拗陷大部分地区隆升成陆,而南羌塘拗陷仍然接受海相沉积,因此,沉积了完整的上三叠统—下侏罗统海相地层,为我国海相T—J界线的研究提供了典型剖面(Hu Fangzhi et al.,2020)。早侏罗世,羌塘盆地发生了大规模的海侵,北羌塘拗陷再次接受海相沉积,形成陆缘近海湖沉积,而南羌塘拗陷大部分地区则为陆棚相沉积(王剑和付修根,2018),记录了典型的早侏罗世托尔期全球大洋缺氧事件(Chen Lan et al.,2005;陈兰等,2007;Fu Xiugen et al.,2014,2016)。早白垩世,受班公湖—怒江洋关闭的影响,羌塘盆地发生了大规模海退,海水逐渐从北羌塘拗陷的西北部退出,南羌塘大部分地区结束了海相沉积,而北羌塘地区则形成了一个向北西开口的巨大海湾(王剑和付修根,2018),记录了典型的早白垩世巴雷姆大洋缺氧事件(Fu Xiugen et al.,2020)。本文对这些重大地质事件研究的最新进展进行了综述,一方面对全球关注的这些重大地质事件在国内的研究进展进行介绍,另外一方面,为我国开展中生代全球重大缺氧事件的研究提供新的思路。

1 地质背景

羌塘盆地位于藏北地区,盆地北部以可可西里—金沙江缝合带为界,南部以班公湖—怒江洋缝合带为界,盆地可再分为北羌塘拗陷、南羌塘拗陷和中央隆起带三个次级构造单元(图1)。晚三叠世,

注:本文为国家自然科学基金资助项目(编号:91955204)和第二次青藏高原科学考察研究计划(STEP)(编号:2019QZKK080301)的成果。
收稿日期:2020-07-10;改回日期:2020-08-20;责任编辑:刘志强。Doi:10.16509/j.georeview.2020.05.004
作者简介:付修根,男,1976年生,博士,教授,主要从事沉积学、油气地质学及事件地质学研究;Email:fuxiugen@126.com。

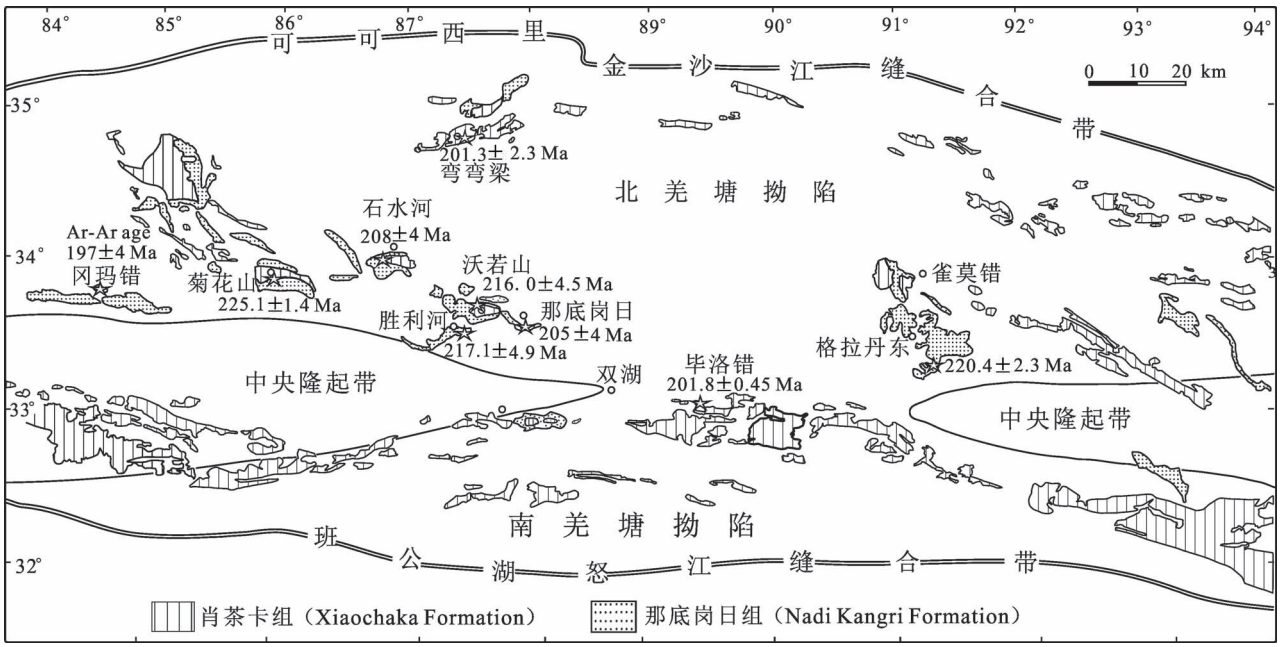

图 1 羌塘盆地次级构造单元及上三叠统地层分布

Fig. 1 Secondary units of the Qiangtang Basin and Upper Triassic strata of the basin

受盆地南部中特提斯洋盆快速开启的影响,盆地内发生了大规模的火山喷发及火山沉积事件,形成具有伸展背景的那底岗日组火山—火山碎屑岩沉积(Wang Jian et al., 2008; Fu Xiugen et al., 2010)。最新的野外地质调查表面,在北羌塘拗陷及中央隆起带均发现有区域性展布的古风化壳(王剑等, 2010),那底岗日组火山—火山碎屑岩沉积超覆在这些古风化壳之上,二者间存在明显的沉积间断(付修根等, 2007)。因此,那底岗日组火山—火山碎屑岩沉积标志着新一轮盆地演化的开始。

盆地内现今出露的地层主要为侏罗纪海相地层,广泛分布于北羌塘拗陷和南羌塘拗陷,自下而上包括下侏罗统曲色组(J_1q)或下—中侏罗统雀莫错组($J_{1-2}q$)、中侏罗统色哇组(J_2s)、布曲组(J_2b)、夏里组(J_2x)、上侏罗统索瓦组(J_3s)和下白垩统白龙冰河组(K_1b)(对应于陆相雪山组地层,K_1x)。而古生代地层则主要见于中央隆起带(王剑等,2004)。最近的一些研究认为,位于羌塘盆地中央隆起带的龙木错—双湖带是青藏高原 3 条主要的晚三叠世板块缝合带之一(李才等, 2007a; Pan Guitang et al., 2012; Metcalfe, 2013; Zhang Xiuzheng et al., 2016)。然而,新的研究显示,中央隆起带即使作为古特提斯洋的洋盆,其规模也并不大(Fan Jianjun et al., 2017),并不可能作为古特提斯洋的主洋盆。

2　三叠纪—侏罗纪之交地层时代的确定及海相 T—J 界线

2.1　三叠纪—侏罗纪之交地层时代的确定

三叠纪—侏罗纪之交,北羌塘拗陷大部分地区表现为雀莫错组冲洪积相沉积超覆在那底岗日组火山—火山碎屑岩地层之上,而南羌塘拗陷则表现为连续的碳酸盐岩沉积,前人的研究中,由于对那底岗日组及其上覆地层时代的认识不清,导致了南北羌塘的地层序列不能准确地对比。

早期的研究中,人们注意到那底岗日组地层被雁石坪群下部砂岩整合覆盖,依据两个相关的同位素测年数据,将其归为雁石坪群下部,即早侏罗世(郝子文和饶荣标,1999),青藏油气勘探项目经理部于咸水河、菊花山、虾河等地采用 Rb-Sr 法和 K-Ar 法所获得的那底岗日组火山岩时代也为早侏罗世或中侏罗世(朱同兴等,2012)。最新的 1∶25 万地质调查结果也显示,位于冈玛错、胜利河等地的那底岗日组火山岩时代为早侏罗世(朱同兴等,2012;牟世勇等,2017)。

然而,事实可能并非如此,这是因为前人对那底岗日组地层的定年常采用 Rb-Sr 法和 K-Ar 法,获得的年龄可能偏年轻。近年来,在那底岗日组年代学的研究方面取得了新的进展。在盆地西部的菊花山

地区,翟庆国和李才(2007)在菊花山剖面采用 SHRIMP 锆石 U-Pb 定年确定的那底岗日组底部年龄为 219±4 Ma,付修根等(2008)在该剖面获得的英安质凝灰岩 SHRIMP 锆石 U-Pb 年龄为 225.1±1.4 Ma;石水河地区,离那底岗日组底部约 256 m(剖面厚度 654 m)获得一件英安岩 SHRIMP 锆石 U-Pb 年龄为 208±4 Ma(王剑等,2007);冈玛错地区,辉绿岩角闪石^{40}Ar-^{39}Ar 年龄为 197±4 Ma(付修根等,2010)。在盆地中部的果干加年山地区(中央隆起带),李才等(2007b)在羌塘盆地采用 SHRIMP 锆石 U-Pb 定年确定的望湖岭组(那底岗日组对应地层)年龄为 214±4 Ma;沃若山地区,离那底岗日组底部约 12 m 获得一件凝灰岩 SHRIMP 锆石 U-Pb 年龄为 216.1±4.5 Ma(王剑等,2008),剖面顶部,获得凝灰岩角闪石^{40}Ar-^{39}Ar 年龄为 201±4 Ma(Hu Fangzhi et al., 2020);那底岗日地区,离那底岗日组顶部约 230 m 和约 150 m 获得两件流纹质凝灰岩 SHRIMP 锆石 U-Pb 年龄为 205±4 Ma 和 210±4 Ma(王剑等,2007);胜利河地区,离那底岗日组底部约 125 m 获得一件英安岩 SHRIMP 锆石 U-Pb 年龄为 217.1±4.9 Ma(付修根等,2010)。在羌塘盆地东部的格拉丹东地区,离那底岗日组底部约 10 m(剖面厚度 776 m)获得一件玄武岩 SHRIMP 锆石 U-Pb 年龄为 220.4±2.3 Ma(Fu Xiugen et al., 2010);李莉等(2012)在该地区那底岗日组上部,确定的那底岗日组年龄为 212.0±1.7 Ma;Li Xueren 等(2018)采用 LA—MC—ICP MS 锆石 U-Pb 定年,确定的那底岗日组地层年龄为 201~225 Ma。在羌塘盆地北部的弯弯梁地区,在那底岗日组顶部获得一件流纹岩 SHRIMP 锆石 U-Pb 年龄为 201.3±0.4 Ma(Hu Fangzhi et al., 2020)。在南羌塘拗陷的毕洛错地区,在那底岗日组顶部获得一件玄武岩 SHRIMP 锆石 U-Pb 年龄为 201.8±0.45 Ma(Fu Xiugen et al., 2016)。上述资料表面,羌塘盆地那底岗日组地层时代为晚三叠世,年龄为 201~225 Ma(图 1),而不是前人归属的早侏罗世或中侏罗世。

在北羌塘拗陷,那底岗日组地层之上沉积了一套以冲洪积相为主的雀莫错组地层,由于下部缺乏生物化石,长期以来对该套地层时代存在较大争议。早期的研究认为,北羌塘拗陷缺失下侏罗统地层,雀莫错组地层时代归属为中侏罗世(郝子文和饶荣标,1999),Yan Maodu 等(2016)和 Fang Xiaomin 等(2016)依据雀莫错组中上部的腕足和双壳化石,将其时代归属为中侏罗世。然而,上述认识并没有准确的同位素年龄,其采用的双壳和腕足化石跨时较大,难以准确地限定雀莫错组地层的时代。最近,在北羌塘拗陷中部的半岛湖地区实施了一口油气科学钻探井(羌科-1 井;付修根等,2020),钻遇了完整的雀莫错组地层(井深 2501~4058 m),该套地层与下伏上三叠统地层为连续地层,这一新认识为雀莫错组地层时代提供了可靠的依据。钻井资料显示,半岛湖地区雀莫错组底部为凝灰质粉砂岩,显示陆缘近海湖沉积的特征,其下伏那底岗日组地层为沉凝灰岩,二者间为整合接触。依据那底岗日组地层时代,推测雀莫错组底部时代归属为早侏罗世。值得注意的是,在雀莫错组三段下部,识别出了早侏罗世托儿期典型的碳同位素负偏异常(3358~3164 m,未发表成果),其特征能够与南羌塘托儿期碳同位素负偏异常对比,该地区发现有托儿期特征的菊石化石,表明其时代为早侏罗世(Fu Xiugen et al., 2016)。这些新资料显示,雀莫错组地层时代主体应该归属为早侏罗世,而不是前人归属的中侏罗世。考虑到雀莫错组上部地层目前尚未发现充分的时代归属证据,本文沿用前人资料。

2.2 海相 T—J 界线及全球对比

三叠纪—侏罗纪之交,南羌塘拗陷沉积了连续的海相碳酸盐岩,为海相 T—J 界线的研究及全球对比提供了典型的剖面。

剖面位于双湖县色哇乡的温泉地区,岩性主要为含生物碎屑灰岩、泥灰岩、含生物碎屑内碎屑灰岩、含生物碎屑微晶灰岩及泥微晶灰岩,剖面中下部含丰富的生物化石,主要包括双壳纲、腕足纲、腹足纲、海胆纲、海百合纲、海绵动物门、藻类及有孔虫纲。依据古生物化石(如菊石亚纲、双壳纲、腕足纲和海绵动物门)、地层层序特征及火山岩年龄等,将研究的索布查组(T_3—J_1s)地层时代归属为晚三叠世—早侏罗世(Hu Fangzhi et al., 2020)。

Hu Fangzhi 等(2020)等对温泉剖面开展了高精度碳同位素分析,研究表明,温泉剖面记录了两次明显的碳同位素负偏,第一次发生在第 6 m 处,偏移幅度为 1.2‰,跨越厚度为 1.5 m(6~7.5 m),第二次发生在 16.7 m 处,偏移幅度远大于第一次的负偏移量,约为 3.4‰,跨越厚度为 3.4 m(16.7~20.0 m)(图 2)。通常来说,无机碳同位素的变化受区域和/或全球事件以及局部古环境条件的控制(Colombié et al., 2011; Lézin et al., 2013);全球事件或区域性事件控制了无机碳同位素的大范围变化,而局部古环境的条件控制了这些大范围变化的幅度(Lézin

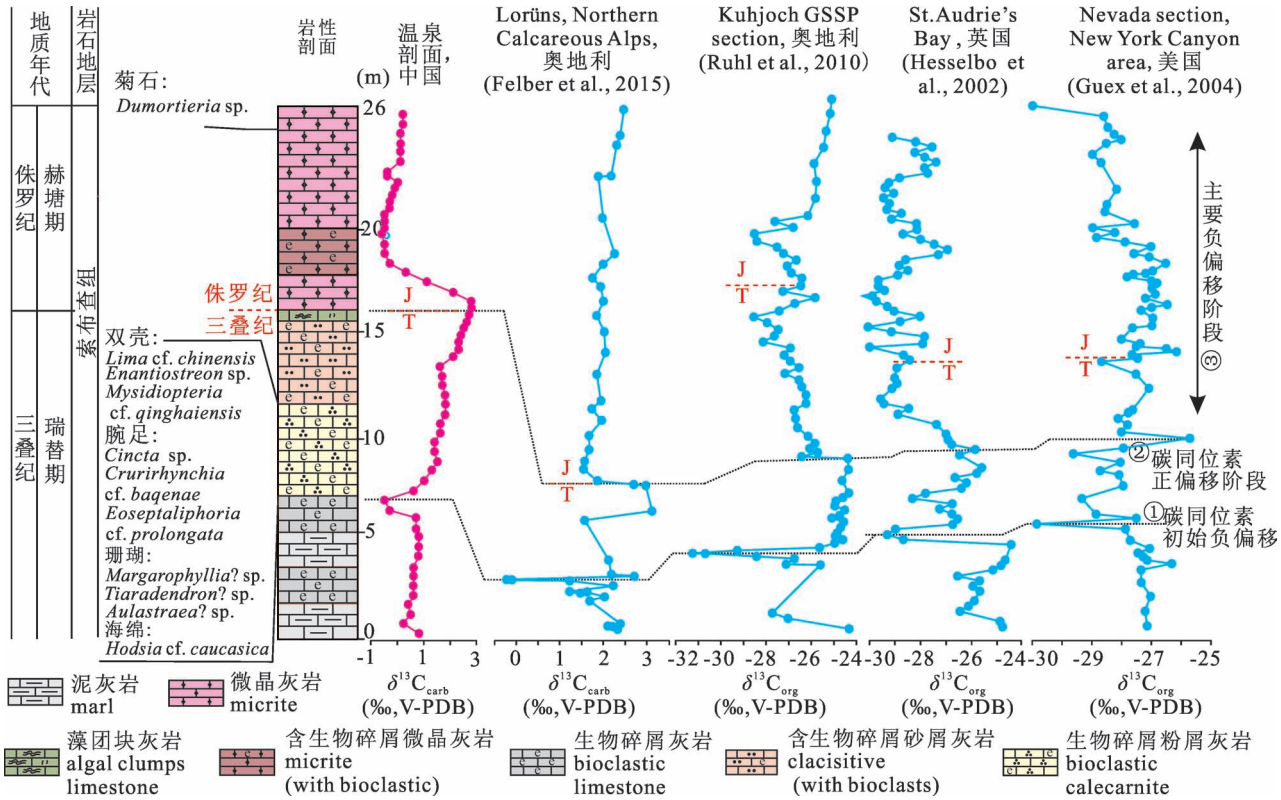

图 2 羌塘盆地温泉 T—J 界线剖面岩石特征、碳同位素剖面及对比(修改自 Hu Fangzhi et al., 2020)

Fig. 2 Lithology and carbon-isotope profile from Wenquan section in the Qiangtang Basin, and a comparison between the $\delta^{13}C_{carb}$ data from the marine T—J boundary in various areas (modified from Hu Fangzhi et al., 2020)

et al., 2013)。温泉剖面中,不同岩性的碳同位素值相近(如剖面底部的泥灰岩和生物碎屑灰岩,图 2);相同氧化—还原条件下碳同位素值表现为较大的差异(如两次负偏均发生在相同的氧化—还原条件下,见下文)。这些特征进一步表明,局部古环境条件并不能控制无机碳同位素的大范围变化。温泉剖面地层中记录的两次碳同位素负偏与全球其他地区晚三叠世—早侏罗世转换之交识别的碳同位素"初始负偏移"和"主要负偏移"能够很好地对应。在奥地利的 Kuhjoch 全球 T—J 界线层型剖面,碳同位素显示两次明显的负偏(Ruhl et al., 2010),在该剖面,碳同位素的"初始负偏移"可与温泉剖面的第一次碳同位素负偏相对比,碳同位素的"主要负偏移"可与温泉剖面的第二次碳同位素负偏相对比(图 2)。T—J 之交的两次碳同位素负偏,在全球的其他地方也被广泛地识别,如英国的 St Audrie's Bay 剖面 (Hesselbo et al., 2002),奥地利的 Lorüns 剖面(Felbe et al., 2015),美国内华达州的 Nevada Muller Canyon 剖面(Guex et al., 2004)等。因此,羌塘盆地温泉地区海相 T—J 界线的碳同位素曲线可与全球其他地区海相 T—J 界线的碳同位素相对比,是全球碳循环的反映(Hu Fangzhi et al., 2020)。

本文对温泉剖面开展了详细的沉积古环境研究,结果表明,温泉剖面底部(0~7 m)为薄层状泥灰岩及含生物化石灰岩,生物化石保存良好、壳薄、中等大小(1~2 cm),草莓状黄铁矿平均粒径为 7.6~8.58 μm。草莓状黄铁矿形成于沉积过程中的准同生时期和成岩作用早期。沉积同生时期的草莓状黄铁矿粒径较小,大小均一,粒径分布范围较窄,这是因为硫化的水体环境为它的生长提供了充足的单质硫、硫化和氢亚铁离子,使得草莓状黄铁矿的成核率大于它的结晶速率从而形成莓状体;而成岩期的草莓状黄铁矿往往粒径较大,大小混杂且粒径分布范围也较广,这是因为氧化的水体环境无法为它的生长提供充足的物质来源从而延长了它的生长时间(Wilkin and Arthur, 2001)。Wilkin 和 Arthur (2001)和 Wei Hengye 等(2015)认为草莓状晶体的平均粒径>6 μm,且颗粒直径变化范围较广,大小混杂,最大直径>18 μm,则表明其形成于成岩期次氧化或氧化的条件;平均粒径<6 μm 且颗粒直径变化

范围较小,大小均一,最大的莓球体直径相对较小<13 μm,则反映了同生期还原的水体环境。温泉剖面底部相对较大粒径草莓状黄铁矿特征指示了偏氧化的环境(Wignall and Newton, 1998),因此,剖面下部被解释为浅海陆棚相沉积。泥灰岩地层之上,沉积了一套含生物碎屑砂屑灰岩,含丰富的底栖有孔虫类(如 *Pachyphloia*, *Globivalvulina*, *Nodosaria* 等, Hu Fangzhi et al., 2020)、腕足类、双壳类、腹足类、珊瑚、海胆类、海百合茎和海绵类等,该套地层中草莓状黄铁矿缺乏,发现的草莓状黄铁平均粒径为 8.4~11.2 μm,这种相对缺乏草莓状黄铁矿的特征指示了氧化的环境(Wignall and Newton, 1998),解释为台地边缘浅滩相沉积。砂屑灰岩之上,沉积了一套粉砂屑灰岩,分选差,结构成熟度低,颗粒间充填泥微晶基质,发现遗迹化石和丰富的生物碎屑,该套地层中草莓状黄铁矿较少,仅在一件样品中发现草莓状黄铁矿,平均粒径为 7.88 μm,指示偏氧化的环境,解释为开阔台地相沉积。粉砂屑灰岩之上,沉积了一套厚度较小的藻团块状微晶灰岩,生物极少,泥微晶基质,该套地层中发现大量的草莓状黄铁矿,平均粒径为 4.86 μm,这种含大量较小粒径草莓状黄铁矿的特征指示了还原的环境(Wignall and Newton, 1998),解释为局限台地相沉积。上述特征总体上反映了水体变浅的特征,结合该时期羌塘盆地为伸展的构造背景,这种特征解释为主要受海平面变化的控制,与羌塘盆地晚三叠世的海退特征一致(王剑等,2004)。

温泉剖面上部(>16.1 m)由中薄层状微晶灰岩和含生物碎屑微晶灰岩组成。16.1~16.7 m 为微晶灰岩,未见生物化石,见一定含量的草莓状黄铁矿,平均粒径为 5.90 μm,指示还原的环境。微晶灰岩之上为含生物碎屑微晶灰岩(16.7~20 m),该套地层中生物化石较少,相对剖面下部生物的个体更小,壳更薄,生物多样性也明显较少,表现出深水动物化石的特征,草莓状黄铁矿丰富,平均粒径为 4.78~6.42 μm,指示次氧化—还原的环境。在 20 m 之上的微晶灰岩中,未发现任何颗粒及生物碎屑,表明沉积区水体已经转变为深水环境,草莓状黄铁矿丰富,平均粒径为 5.40~7.31 μm,指示次氧化—还原的环境。因此,剖面上部解释为浅海陆棚相沉积,结合该时期羌塘盆地为伸展的构造背景,这种特征可能受区域构造和海平面变化的共同控制。早侏罗世时期,羌塘盆地总体表现为向上变深的海侵序列(王剑等,2004)。

上述研究表明,温泉剖面下部地层(0~16.1 m)表现为明显的海退序列,上部地层(>16.1 m)表现为明显的海侵序列,这不仅与羌塘盆地晚三叠世—早侏罗世之交的海平面变化一致,而且可与全球晚三叠世—早侏罗世转换期海平面变化相对比(Miller et al., 2005)。其转换界面可作为区域对比的标志,该界面也代表了 T—J 的转换界线。剖面古生物地层研究表面,界面之上地层中发现了菊石 *Dumortieria* sp.(Hu Fangzhi et al., 2020),该菊石广泛见于伊朗厄尔布尔士东南部 Shahmirzad 地区的下托尔阶 *Dumortieria pseudoradiosa* 带(Seyed-Emami et al., 2008),保加利亚托尔阶的 *Dumortieria pseudoradiosa* 带(Metodiev, 2008),欧洲西北部托尔阶的 *Levesquei* 亚带(Elmi et al., 1997),因此,界面之上地层时代归属为早侏罗世。界面之下地层中见有晚三叠世的双壳类(*Enantiostreon* sp., *Lima* cf. *chinensis*, *Mysidiopteria* cf. *qinghaiensis*),腕足类(*Crurirhynchia* cf. *baqenae*, *Cincta* sp., *Eoseptaliphoria* cf. *prolongata*),珊瑚(*Aulastraea*? sp., *Tiaradendron*? sp., *Margarophyllia*? sp.)和海绵类(*Hodsia* cf. *caucasica*)化石,时代归属为晚三叠世。另外,区域地层对比表面,转换界面的时间为~201 Ma(Hu Fangzhi et al., 2020),因此,羌塘盆地海相 T—J 的界线年龄为 201 Ma。

3 早侏罗世托儿期缺氧事件及对比

早侏罗世托尔期全球大洋缺氧事件(Toarcian Oceanic Anoxic Event, T-OAE)是侏罗纪最有意义和最广泛的黑色页岩沉积事件之一(Jenkyns, 1988; Cohen et al., 2007; Kemp et al., 2019)。该套黑色页岩的沉积,与全球海洋生态系统的扰动(Mattioli et al., 2009; Reolid et al., 2019)以及气候的快速变化一致(Izumi et al., 2018; Fantasia et al., 2019)。T-OAE 表现为碳同位素的大幅度(2‰~7‰)快速负偏,这种碳同位素异常不仅在海相生态系统中被广泛识别,而且,在陆相源区的生物标志物以及化石中也被广泛识别(McElwain et al., 2005; Hessebo and Pieńkowski, 2011),表明了该事件对大气 CO_2 库的影响。因此,托尔期缺氧事件可能是一次全球性事件(Hesselbo et al., 2000; Kemp et al., 2019)。

近年来,东特提斯地区早侏罗世托尔期全球缺氧事件的研究取得了一定的进展,但是,这些研究仅限于南羌塘拗陷的有限剖面。尽管在藏南地区也发

现了托尔期的碳同位素异常剖面(Han Zhong et al., 2018),但在早侏罗世时期,藏南属于南半球。羌塘盆地属于特提斯构造域的东段北部,是连接欧洲特提斯及东南亚特提斯的关键区域。南羌塘拗陷下侏罗统为曲色组,岩性为一套黑色页岩夹灰岩地层,见有大量的菊石、腕足类和双壳类化石。在南羌塘毕洛错地区,伊海生等(2003)较早地识别出了托尔期的菊石,22 个菊石属保存较好,但菊石属非常单一,其特征与托尔期的 *Harpoceras* sp. 一致。另外,菊石 *Cleviceras* cf. *elegans* 也在该地区被采集到(阴家润等, 2006),对应于巴黎盆地的 *Harpocearas falciferum* 带,也能够与欧洲其他地方下托尔阶地层相对比(Chen Lan et al., 2005; Fu Xiugen et al., 2016)。在毕洛错地区,还发现有菊石 *Dactylioceras* sp. 和 *Dactylioceras* cf. *directum* (Buckman),这些菊石伴随着丰富的双壳化石 *Bositra buchi*。这些菊石和双壳能够大致地对应于泛大洋西部的 *Dactylioceras tenuicostatum* 带 (Hesselbo et al., 2007)。

尽管取得了上述进展,但问题仍然存在,一个重要的方面在于采集的菊石化石单一,而且,这些菊石化石主要采自路线剖面,不能很好地在实测剖面上标定准确的位置。近年来,对羌塘盆地毕洛错剖面进行了详细研究,取得了重要进展。剖面位于南羌塘毕洛错地区(毕洛错剖面),剖面中下部为膏岩、泥灰岩、钙质泥岩组合,化石稀少,显示明显的封闭环境沉积特征,气候条件为干旱炎热,蒸发作用强烈(Fu Xiugen et al., 2017)。剖面中部为钙质泥岩、泥质灰岩与薄层石膏互层,由于海平面的频繁升降(王剑等,2004),盐度波动大,发育内栖双壳为主的动物群,总体上表现为海侵特征。剖面上部为一套页岩(油页岩)为主的沉积,夹少量泥晶灰岩(图 3)。本文对剖面上部地层开展了详细研究,在页岩底部,采集了一件碎屑岩样品,其 21 颗最年轻锆石(次棱角—棱角状)年龄为 184.4 ± 0.6 Ma (Fu Xiugen et al., 2016),代表了该套碎屑岩的最大沉积年龄,表明了该套地层沉积年龄为早侏罗世。

近年来,对毕洛错页岩(油页岩)沉积古水体环境研究也取得了新进展,研究揭示毕洛错页岩中还原敏感的微量元素 U 和 V 具有中等富集的特征,富集系数($EF=(X/\mathrm{Al})_{\mathrm{sample}}/(X/\mathrm{Al})_{\mathrm{PAAS}}$,$X$ 代表元素,PAAS 为澳大利亚后太古平均页岩)分别为 3.02 和 1.27,还原敏感的微量元素 Mo 具有高度富集的特

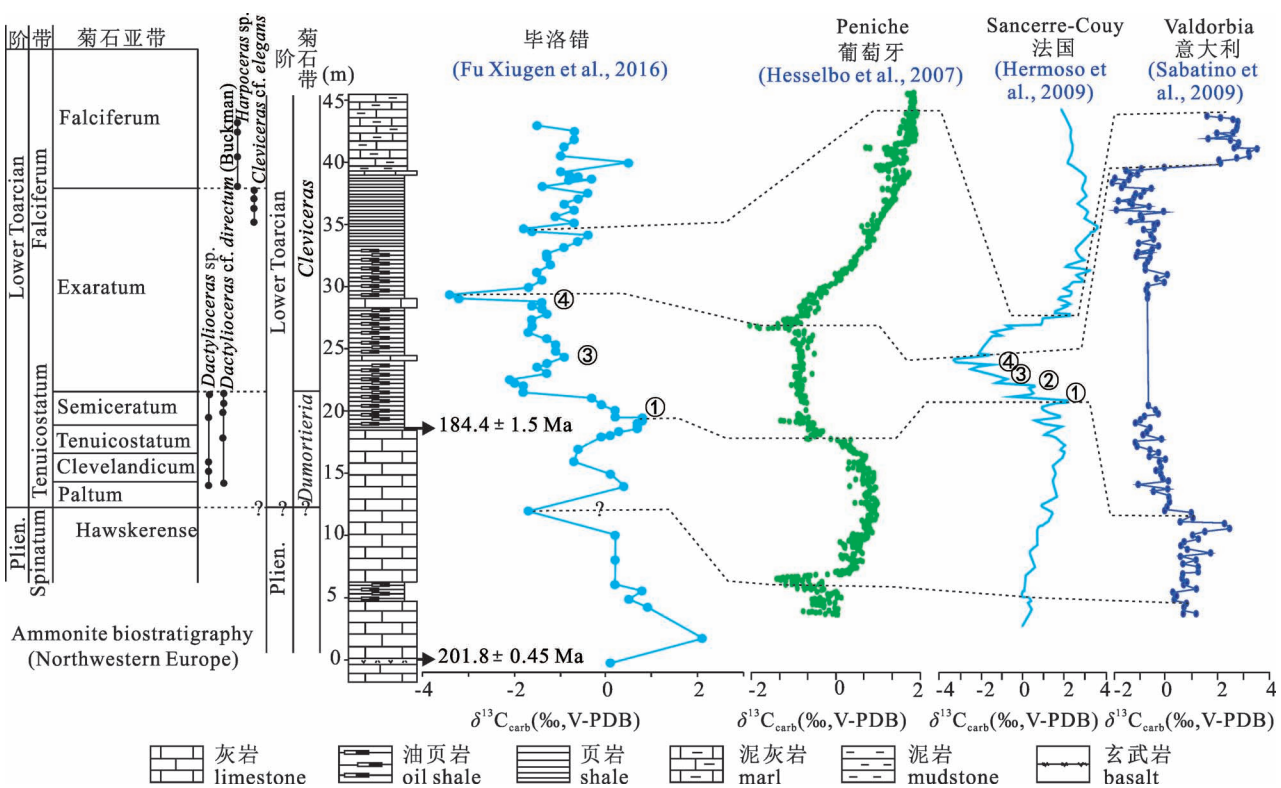

图 3 羌塘盆地毕洛错剖面岩性特征、碳同位素剖面及对比(修改自 Fu Xiugen et al., 2016)

Fig. 3 Lithology and carbon-isotope profile from Bilong Lake section in the Qiangtang Basin, and a comparison between the $\delta^{13}C_{carb}$ data from the Early Toarcian strata in various areas (modified from Fu Xiugen et al., 2016)

征,富集系数为 36.2(Fu Xiugen et al., 2017)。Tribovillard 等(2006)建议,当有机质含量高于某个门限时,Mo 的富集伴随着 U 和 V 的富集,表明了缺氧(静水)的水体环境。这一解释与页岩 C_{org} : P 比率获得的结果一致,研究表明样品的 C_{org} : P 比率为 221~346(Fu Xiugen et al., 2017),显示明显的缺氧环境的特征。矿物学特征研究表明,毕洛错页岩(油页岩)中发现大量草莓状黄铁矿,这些黄铁矿颗粒较小,大多小于 0.5 μm(Fu Xiugen et al., 2017),指示页岩(油页岩)沉积期为缺氧的水体环境。

这些研究表明,毕洛错页岩(油页岩)形成于缺氧的水体环境,有机质含量高(1.45%~14.1%,Fu Xiugen et al., 2017),其最大沉积年龄为 184.4±0.6 Ma(Fu Xiugen et al., 2016)。这可能与早侏罗世托儿期全球大洋缺氧事件有关。碳同位素研究表明,碳同位素在大约 184 Ma 发生了明显的负偏(图 3),偏移幅度分别为 2.6‰和 1.9‰(Fu Xiugen et al., 2016),这一特征可与德国的 Dotternhausen(Röhl et al., 2001),威尔士的 Mochras(Jenkyns et al., 2001)和英国的 Yorkshire(Kemp et al., 2005)相对比,表明毕洛错地区的缺氧事件可能是早侏罗世托儿期全球大洋缺氧事件在该地区的反映。

4 早白垩世巴雷姆期缺氧事件及对比

4.1 羌塘盆地下白垩统地层沉积特征及时代的确定

前人对羌塘盆地的地层研究认为,羌塘盆地普遍缺失下白垩统地层,然而,谭富文等(2004)在最初定义的羌塘盆地上侏罗统地层中发现晚侏罗世—早白垩世化石分子,因此,提出了上侏罗统—下白垩统的概念。

早白垩世,羌塘盆地海水逐渐从北羌塘拗陷的西北部退出,因此,下白垩统地层主要见于北羌塘拗陷。在该地区,下白垩统地层主要为白龙冰河组灰岩及碎屑岩沉积。白龙冰河组下部,岩性主要为泥晶灰岩夹粉砂岩和生物碎屑灰岩,见有丰富孢粉:*Brevilaesuraspora orbiculata*、*Classopollis* spp.、*C. annulatus*、*C. minor*、*C. classoides*、*Cyathidites minor*、*Cyclogranisporites* sp.、*Densoisporites* sp.、*Dicheiropollis etruscus*、*Osmundacidites* spp.、*Pinuspollenites* sp.、*Perinopollenites* sp.、*Todisporites minor*、*Vitreisporites* sp. 等(朱同兴等, 2012; Fu Xiugen et al., 2020)。这些孢粉中,最明显的特征是出现了早白垩世早期典型的分子 *Dicheiropollis* 花粉,这一孢粉组合中同时还含大量的 *Classopollis*,指示这些孢粉组合时代归属为早白垩世早期。白龙冰河组下部岩石为泥微晶结构,水平层理发育,显示低能的沉积环境。化石组合除了孢粉外,还发现有底栖藻类、菊石化石、双壳类和腕足类化石(Fu Xiugen et al., 2020),这些资料表明沉积于海相环境。在局部地区,泥质沉积与粗粒沉积(生物碎屑灰岩)交替出现,发育流水波痕和透镜状层理(Fu Xiugen et al., 2020),表明受到了潮汐作用的影响。因此,白龙冰河组下段地层可能沉积于半封闭的海湾环境。

白龙冰河组中部岩性主要为页岩(油页岩)、泥晶灰岩、泥灰岩夹生物碎屑灰岩组合。该套地层中同样发现了丰富的孢粉化石,包括:*Apiculatisporites* sp.、*Biretisporites* sp.、*Cerebropollenites* sp.、*C.* cf. *papilloporus*、*Chasmatosporite* sp.、*Cicatricosisporites* sp.、*C. ludbrooki*、*Densosporites* sp.、*Classopollis* sp.、*Ephedripites* cf. *notensis*、*Jiaohepollis* sp.、*Lygodiumsporites subsimplex*、*Perinopollenites* sp.、*Reticulisporites* sp.、*Triporopollenites* sp.、*Tricolporopolenites* sp. 等(朱同兴等,2012;Fu Xiugen et al., 2020)。这些孢粉中,最明显的特征是被子植物花粉 *Triporopollenites* sp. 和 *Tricolporopolenites* sp. 的出现,表明时代归属为早白垩世,另外一些孢粉,包括 *Ephedripites* cf. *notensis*、*Lygodiumsporites subsimplex* 和 *Cicatricosisporites ludbrooki* 的出现也证实了上述认识。值得注意的是,在白龙冰河组中部页岩(油页岩)中获得的 Re-Os 同位素年龄为 124.5±4.3 Ma(Wang Xuance and Li Jie, 2013),表明白龙冰河组中部地层时代归属为早白垩世中期。白龙冰河组中部地层发育水平层理,岩石结构为泥质结构,见有丰富的细小的草莓状黄铁矿,页岩中见有红藻和保存较好的腕足类、双壳类化石,表明该套地层仍然沉积于半封闭的海湾环境,但需要指出的是,与白龙冰河组下部地层相比,中部地层中陆源碎屑明显增加(Fu Xiugen et al., 2020)。

白龙冰河组上部为一套膏岩夹泥灰岩、生物碎屑灰岩的岩石组合,泥灰岩中发现有丰富的孢粉,包括:*Cycadopites* sp.、*C. adjectus*、*C. balmei*、*Classopollis* sp.、*C. annulatus*、*C. classoides*、*C. granulatus*、*C. mino*、*Cyclogranisporites* sp.、*Doltoidospora regularis*、*Lygodiumsporites subsimplex*、*Osmundacidites* spp.、*Senegalosporites* sp.、*Steevesipollenites* sp.、*Waltzispora* sp. 等(朱同兴等,

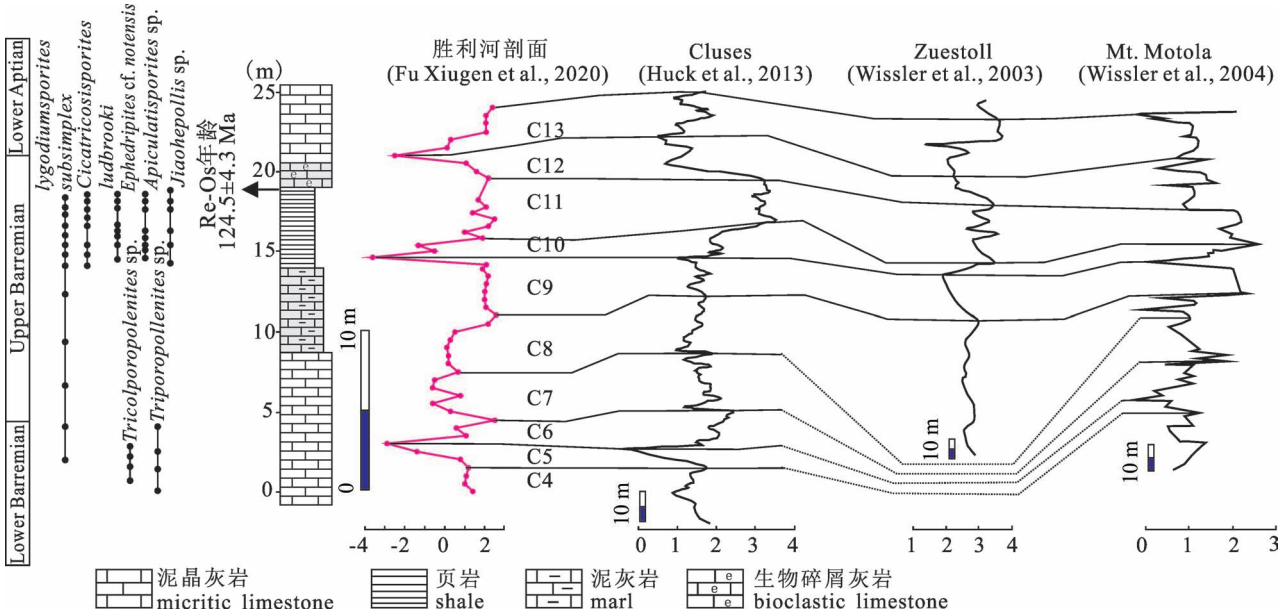

图 4 羌塘盆地胜利河剖面岩性特征、碳同位素剖面及对比(修改自 Fu Xiugen et al., 2020)

Fig. 4 Lithology and carbon-isotope profile from the Shengli River section in the Qiangtang Basin, and a comparison between the $\delta^{13}C_{carb}$ data from the Early Cretaceous strata in various areas (modified from Fu Xiugen et al., 2020)

2012;Fu Xiugen et al., 2020)。这些孢粉中,最明显的特征是 *Steevesipollenites* sp. 和 *Senegalosporites* sp. 的出现,另外,识别出较低含量的 *Lygodiumsporites subsimplex*,表明时代归属为早白垩世,可能为阿尔必阶。该套地层中石膏以层状为主,缺乏暴露标志,分布规模较大(Fu Xiugen et al., 2020),这些资料表明气候干旱炎热,为蒸发台地的环境。

4.2　巴雷姆期缺氧事件及对比

在羌塘盆地,除了在早侏罗世识别出托儿期缺氧事件外,在早白垩世巴雷姆期还识别出缺氧事件(巴雷姆缺氧事件)。研究剖面位于北羌塘胜利河地区,属于白龙冰河组中部,剖面下部为泥晶灰岩,中部为泥灰岩,中上部为页岩(油页岩),顶部为生物碎屑灰岩及泥晶灰岩(图 4)。沉积环境研究表明,胜利河页岩样品中富集还原敏感的元素 U、Mo 和 V,富集系数分别为 32.5、197 和 3.90(Fu Xiugen et al., 2020)。页岩中高的 Mo 富集并伴随着 U 和 V 的富集揭示了沉积期还原的水体环境(可能为静水环境)。胜利河页岩样品显示轻微高的 C_{org} : P 比率(平均 69; Fu Xiugen et al., 2020),也显示了缺氧环境的特征。另外,在胜利河页岩中发育丰富的草莓状黄铁矿,这些黄铁矿粒径大多小于 5 μm (Fu Xiugen et al., 2020),指示页岩沉积期为缺氧的水体环境。

胜利河页岩(油页岩)剖面详细的碳同位素分析表明,碳同位素剖面可以分为 10 段,分别为 C4~C13,其中,C5、C10 和 C12 表现为明显的负偏异常,C7 和 C8 表现为波动性变化,C9 和 C11 为明显的正偏异常(Fu Xiugen et al., 2020)。这些特征可与西北特提斯域巴雷姆期典型剖面的碳同位素特征相对比,记录了巴雷姆期全球大洋缺氧事件。在西北特提斯域的 Cluses 剖面,碳同位素剖面可以分为 13 段(Huck et al., 2013),其中,Cluses 剖面的 C4~C13 段与胜利河剖面的 C4~C13 段能够较好地对比(图 4)。另外,在南特提斯域的 Mt. Motola 剖面(Wissler et al., 2004)、北特提斯域的 Zuestoll 剖面(Wissler et al., 2003),碳同位素也记录了相似的变化特征。因此,巴雷姆期碳同位素异常可能并不是区域性的,而是全球碳循环的反映。在特提斯构造域的中段,大套黑色页岩的形成与巴雷姆全球大洋缺氧事件有关(Huck et al., 2013)。

值得注意的是,在胜利河剖面,确定的页岩沉积年龄约为 124.5±4.3 Ma(Wang Xuance and Li Jie, 2013),这一沉积年龄与早白垩世 Ontong Java 大洋高原火山岩省的火山喷发年龄基本一致(^{40}Ar-^{39}Ar 年龄为 121.3±0.9 Ma; Tejada et al., 1996)。因此,巴雷姆期全球大洋缺氧事件可能与大火山岩省的火山喷发有关。

5 结论

(1)羌塘中生代盆地地层研究取得重要进展,北羌塘地区并不缺失下侏罗统地层,在北羌塘拗陷中部,雀莫错组地层时代主体应该归属为早侏罗世,而不是前人归属的中侏罗世;羌塘盆地存在早白垩世海相沉积,白龙冰河组地层时代归属为早白垩世。

(2)晚三叠世—早侏罗世,羌塘盆地海平面发生了明显的变化,与全球对应时期海平面变化一致;海相 T—J 界线剖面的碳同位素发生了两次碳同位素负偏,与全球其他地区晚三叠世—早侏罗世之交识别的碳同位素"初始负偏移"和"主要负偏移"能够很好地对应;T—J 之交海洋水体环境发生了明显变化,由氧化环境变为缺氧环境。

(3)在羌塘盆地毕洛错地区识别出早侏罗世托儿期碳同位素负偏异常,可与全球早侏罗世托尔期大洋缺氧事件的碳同位素负偏进行精确地对比,羌塘盆地早侏罗世托儿期全球大洋缺氧事件的碳同位素具有突变的特征,该缺氧事件可能是早侏罗世托儿期全球大洋缺氧事件在羌塘盆地的反映。

(4)早侏罗世,北羌塘拗陷为残留海湾沉积,广泛沉积了一套页岩、油页岩及泥岩的岩石组合,形成于缺氧的水体环境,碳同位素特征可与南特提斯、北特提斯及西北特提斯对应时期的碳同位素相对比,该套黑色页岩(油页岩)为早白垩世巴雷姆期全球大洋缺氧事件在羌塘盆地的反映。

致谢:感谢审稿专家和编辑章雨旭研究员提出的宝贵意见。

参 考 文 献 / References

(The literature whose publishing year followed by a "**&**" is in Chinese with English abstract; The literature whose publishing year followed by a "**#**" is in Chinese without English abstract)

陈兰, 伊海生, 夏敏全, 皱艳荣. 2007. 藏北双湖地区早 Toarcian 期大洋缺氧事件: 沉积学、古生物学及地球化学特征. 生态学杂志, 26(11): 1793~1797.

付修根, 王剑, 汪正江, 陈文西. 2007. 藏北羌塘盆地上三叠统那底岗日组与下伏地层沉积间断的确立及意义. 地质论评, 53(3): 329~336.

付修根, 王剑, 汪正江, 陈文西. 2008. 藏北羌塘盆地菊花山地区火山岩 SHRIMP 锆石 U-Pb 年龄及地球化学特征. 地质论评, 54(2): 232~241.

付修根, 王剑, 陈文彬, 冯兴雷. 2010. 羌塘盆地那底岗日组火山岩地层时代及其构造背景研究. 成都理工大学学报(自然科学版), 37(6): 605~615.

付修根, 王剑, 宋春彦, 刘中戎. 2020. 羌塘盆地第一口油气科学钻探井油气地质成果及勘探意义. 沉积与特提斯地质, 40(1): 16~25.

郝子文, 饶荣标. 1999. 全国地层多重划分对比研究—西南区区域地层. 武汉: 中国地质大学出版社: 122.

牟世勇, 熊兴国, 王常薇, 王敏, 陈仁, 曾昌兴, 卢定彪, 岳龙, 易成兴, 贺永忠, 朱勋, 边申武, 徐安全, 况忠, 赵伟立. 2017. 中华人民共和国区域地质调查报告(1:25 万丁固幅). 北京: 地质出版社: 55~58.

李才, 翟庆国, 陈文, 董永胜, 于介江. 2007a. 青藏高原龙木错—双湖板块缝合带闭合的年代学证据—来自果干加年上蛇绿岩与流纹岩 Ar-Ar 和 SHRIMP 年龄制约. 岩石学报, 23(5): 911~918.

李才, 翟庆国, 董永胜, 于介江, 黄小鹏. 2007b. 青藏高原羌塘中部果干加年山上三叠统望湖岭组的建立及意义. 地质通报, 26(8): 1003~1008.

李莉, 牛志军, 白云山, 姚华舟, 段其发. 2012. 长江源各拉丹冬一带晚三叠世那底岗日组. 地层学杂志, 36(1): 49~54.

谭富文, 王剑, 李永铁, 杜佰伟, 朱忠发. 2004. 羌塘盆地侏罗纪末—早白垩世沉积特征与地层问题. 中国地质, 31(4): 400~405.

王剑, 谭富文, 李亚林, 李永铁, 陈明, 王成善, 郭祖军, 王小龙, 杜佰伟, 朱忠发. 2004. 青藏高原重点沉积盆地油气资源潜力分析. 北京: 地质出版社: 34~88.

王剑, 汪正江, 陈文西, 付修根, 陈明. 2007. 藏北北羌塘盆地那底岗日组时代归属的新证据. 地质通报, 26(4): 404~409.

王剑, 付修根, 陈文西, 谭富文, 汪正江, 陈明, 卓皆文. 2008. 北羌塘沃若山地区火山岩年代学及区域地球化学对比——对晚三叠世火山—沉积事件的启示. 中国科学(D 辑):地球科学, 38(1): 33~43.

王剑, 付修根, 谭富文, 陈明, 何江林. 2010. 羌塘中生代(T_3—K_1)盆地演化新模式. 沉积学报, 28(5): 884~893.

王剑, 付修根. 2018. 论羌塘盆地沉积演化. 中国地质, 45(2): 237~259.

伊海生, 林金辉, 赵兵, 李勇, 石和, 朱利东. 2003. 藏北羌塘地区地层新资料. 地质论评, 49: 59~65.

阴家润, 高金汉, 王永胜, 张树岐, 郑春子, 徐德彪, 白志达, 孙立新, 苏新. 2006. 色哇—安多地区侏罗纪菊石类与缺氧黑色页岩相. 古生物学报, 45: 311~331.

翟庆国, 李才. 2007. 藏北羌塘菊花山那底岗日组火山岩锆石 SHRIMP 定年及其意义. 地质学报, 81(6): 795~801.

朱同兴, 冯兴涛, 林仕良, 张正贵, 周铭魁. 2012. 中华人民共和国区域地质调查报告(1: 25 万黑虎岭幅). 北京: 中国地质大学出版社: 24~56.

Chen Lan, Yi Haisheng, Hu Ruizhong, Zhong Hong, Zou Yanrong. 2005. Organic geochemistry of the Early Jurassic oil shale from the Shuanghu area in northern Tibet and the Early Toarcian oceanic anoxic event. Acta Geologica Sinica(English Edition), 79: 392~397.

Chen Lan, Yi Haisheng, Xia Minquan, Zou Yanrong. 2007**&**. Early Toarcian oceanic anoxic event in the Shuanghu area, northern Tibet: Sedimentology, palaeobiology and geochemistry. Chinese Journal of Ecology, 26(11): 1793~1797.

Cohen A S, Coe A L, Kemp D B. 2007. The Late Palaeocene—Early Eocene and Toarcian (Early Jurassic) carbon isotope excursions: a comparison of their time scales, associated environmental changes, causes and consequences. Journal of the Geological Society, 164: 1093~1108.

Colombié C, Lécuyer C, Strasser A. 2011. Carbon- and oxygen-isotope records of palaeoenvironmental and carbonate production changes in shallow-marine carbonates (Kimmeridgian, Swiss Jura). Geological

Magazine, 148: 133~153.

Elmi S, Rulleau L, Gabilly J, Mouterde R. 1997. Toarcien. Biostratigraphie du Jurassique ouest—européen et méditerranéen: Pau. Bulletin du Centre de recherché ELF Exploration Production, mémoire, 17: 25~36.

Fan Jianjun, Li Cai, Xie Chaoming, Liu Yiming, Xu Jianxin, Chen Jingwen. 2017. Remnants of late Permian—Middle Triassic ocean islands in northern Tibet: Implications for the late-stage evolution of the Paleo-Tethys Ocean. Gondwana Research, 44: 7~21.

Fantasia A, Föllmi K B, Adatte T, Spangenberg J E, Montero-Serrano J C. 2019. The Early Toarcian oceanic anoxic event: Paleoenvironmental and paleoclimatic change across the Alpine Tethys (Switzerland). Global and Planetary Change, 162: 53~68.

Fang Xiaoming, Song Chunhui, Yan Maodu, Zan Jinbo, Liu Chenglin, Sha Jingeng, Zhang Wweilin, Zeng Yongyao, Wu Song, Zhang Dawen. 2016. Mesozoic litho- and magneto-stratigraphic evidence from the central Tibetan Plateau for megamonsoon evolution and potential evaporates. Gondwana Research, 37: 110~129.

Felber R, Weissert H J, Furrer H, Bontognali T R R. 2015. The Triassic—Jurassic boundary in the shallow-water marine carbonates from the western northern calcareous Alps (Austria). Swiss Journal of Geosciences, 108 (2~3): 213~224.

Fu Xiugen, Wang Jian, Wang Zhengjiang, Chen Wenxi. 2007&. Identification of sedimentary gap between the Late Triassic Nadi Kangri Formation and its underlying strata in the Qiangtang Basin, northern Xizang (Tibet) and its geological significance. Geological Review, 53(3): 329~336.

Fu Xiugen, Wang Jian, Wang Zhengjiang, Chen Wenxi. 2008&. U-Pb zircon age and geochemical characteristics of volcanic rocks from the Juhua Mountain area in the northern Qiangtang Basin, northern Xizang (Tibet). Geological Review, 54 (2): 232~241.

Fu Xiugen, Wang Jian, Tan Fuwen, Chen Ming, Chen Wenbin. 2010. The Late Triassic rift-related volcanic rocks from eastern Qiangtang, northern Tibet (China): Age and tectonic implications. Gondwana Research, 17(1): 135~144.

Fu Xiugen, Wang Jian, Chen Wenbin, Feng Xinglei. 2010&. Age and tectonic implications of the Late Triassic Nadi Kangri volcanic rocks in the Qiangtang Basin, northern Tibet, China. 37(6): 605~615.

Fu Xiugen, Tan Fuwen, Feng Xinglei, Wang Dong, Chen Wenbin, Song Chunyan, Zeng Shengqiang. 2014. Early Jurassic anoxic conditions and organic accumulation in the eastern Tethys. International Geology Review, 56(12): 1450~1465.

Fu Xiugen, Wang Jian, Chen Wenbin, Feng Xinglei, Wang Dong, Song Chunyan, Zeng Shengqiang. 2015. Organic accumulation in lacustrine rift basin: constraints from mineralogical and multiple geochemical proxies. International Journal of Earth Sciences, 104: 495~511.

Fu Xiugen, Wang Jian, Feng Xinglei, Wang Dong, Chen Wenbin, Song Chunyan, Zeng Shengqiang. 2016. Early Jurassic carbon-isotope excursion in the Qiangtang Basin (Tibet), the eastern Tethys: Implications for the Toarcian Oceanic anoxic event. Chemical Geology, 442: 62~72.

Fu Xiugen, Wang Jian, Zeng Shengqiang, Feng Xinglei, Wang Dong, Song Chunayn. 2017. Continental weathering and palaeoclimatic changes through the onset of the Early Toarcian oceanic anoxic event in the Qiangtang Basin, eastern Tethys. Palaeogeography, Palaeoclimatology, Palaeoecology, 487: 241~250.

Fu Xiugen, Wang Jian, Song Chunyan, Liu Zhongrong. 2020&. Petroleum geological achievements and exploration significance of the first oil and gas scientific drilling well in the Qiangtang Basin. Sedimentary Geology and Tethyan Geology, 40(1): 16~25.

Fu Xiugen, Wang Jian, Wen Huaguo, Wang Zhongwei, Zeng Shengqiang, Song Chunyan, Wang Dong, Nie Ying. 2020. Carbon-isotope record and paleoceanographic changes prior to the OAE 1a in the Eastern Tethys: Implication for the accumulation of organic-rich sediments. Marine and Petroleum Geology, 113: 104049.

Guex J, Bartolini A, Atudorei V, Taylor D. 2004. High-resolution ammonite and carbon isotope stratigraphy across the Triassic—Jurassic boundary at New York Canyon (Nevada). Earth and Planetary Science Letters, 225 (1~2): 29~41.

Hao Zhiwen, Rao Rongbiao. 1999#. Research on multiple stratigraphic division and correlation: regional stratigraphy in Southwest area. Wuhan: China University of Geosciences Press, 122.

Han Zhong, Hu Xiumian, Kemp D B, Li Juan. 2018. Carbonate-platform response to the Toarcian Oceanic Anoxic Event in the southern hemisphere: Implications for climatic change and biotic platform demise. Earth and Planetary Science Letters, 489: 59~71.

Hermoso M, Le Callonnec L, Minoletti F, Renard M, Hesselbo S P. 2009. Expression of the Early Toarcian negative carbon-isotope excursion in separated carbonate microfractions (Jurassic, Paris Basin). Earth and Planetary Science Letters, 277: 194~203.

Hesselbo S P, Gröcke D R, Jenkyns H C, Bjerrum C J, Farrimond P, Morgans Bell H S, Green O R. 2000. Massive dissociation of gas hydrate during a Jurassic oceanic anoxic event. Nature, 406: 392~395.

Hesselbo S P, Jenkyns H C, Duarte L V, Oliveira L C V. 2007. Carbon-isotope record of the Early Jurassic (Toarcian) Oceanic Anoxic Event from fossil wood and marine carbonate (Lusitanian Basin, Portugal). Earth and Planetary Science Letters, 253: 455~470.

Hesselbo S P, Pieńkowski G. 2011. Stepwise atmospheric carbon-isotope excursion during the Toarcian Oceanic Anoxic Event (Early Jurassic, Polish Basin). Earth and Planetary Science Letters, 301: 365~372.

Hesselbo S P, Robinson S A, Surlyk F, Piasecki S. 2002. Terrestrial and marine extinction at the Triassic—Jurassic boundary synchronized with major carbon-cycle perturbation: a link to initiation of massive volcanism? Geology, 30 (3): 251~254.

Hu Fangzhi, Fu Xiugen, Lin iL, Song Chunayn, Wang Zhongwei, Tian Kangzhi. 2020. Marine Late Triassic—Jurassic carbon-isotope excursion and biological extinction records: New evidence from the Qiangtang Basin, eastern Tethys. Global and Planetary Change, 2020, 185: 103093.

Huck S, Heimhofer U, Immenhauser A, Weissert H. 2013. Carbon-isotope stratigraphy of Early Cretaceous (Urgonian) shoal-water deposits: Diachronous changes in carbonate-platform production in the north-western Tethys. Sedimentary Geology, 290: 157~174.

Izumi K, Endo K, Kemp D B, Inui M. 2018. Oceanic redox conditions through the late Pliensbachian to early Toarcian on the northwestern Panthalassa margin: Insights from pyrite and geochemical data. Palaeogeography, Palaeoclimatology, Palaeoecology, 493: 1~10.

Jenkyns H C. 1988. The Early Toarcian (Jurassic) anoxic event —— stratigraphic, sedimentary, and geochemical evidence. American Journal of Science, 288: 101~151.

Jenkyns H C, Gröcke D R, Hesselbo S P. 2001. Nitrogen isotope

evidence for water mass denitrification during the Early Toarcian (Jurassic) oceanic anoxic event. Paleoceanography, 16: 593~603.

Kemp D, Baranyi V, Kentaro I, Burgess R D. 2019. Organic matter variations and links to climate across the early Toarcian oceanic anoxic event (T-OAE) in Toyora area, southwest Japan. Palaeogeography, Palaeoclimatology, Palaeoecology, 530: 90~102.

Kemp D B, Coe A L, Cohen A S, Schwark L. 2005. Astronomical pacing of methane release in the Early Jurassic period. Nature, 437: 396~399.

Kemp D B, Izumi K. 2014. Multiproxy geochemical analysis of a Panthalassic margin record of the early Toarcian oceanic anoxic event (Toyora area, Japan): Palaeogeography Palaeoclimatology Palaeoecology, 414: 332~341.

Lézin C, Andreu B, Pellenard P, Bouchez J L, Emmanuel L, Fauré P, Landrein P. 2013. Geochemical disturbance and paleoenvironmental changes during the Early Toarcian in NW Europe. Chemical Geology, 341: 1~15.

Li Cai, Zhai Qingguo, Chen Wen, Dong Yongsheng, Yu Jiejiang. 2007a&. Geochronology evidence of the closure of Longmu CoShuanghu suture, Qinghai—Tibet plateau: Ar-Ar and zircon SHRIMP geochronology from ophiolite and rhyolite in Guoganjianian. Acta Petrologica Sinica, 23(5): 911~918.

Li Cai, Zhai Qingguo, Dong Yongsheng, Yu Jiejiang, Huang Xiaopeng. 2007b&. Establishment of the Upper Triassic Wanghuling Formation at Guoganjianian Mountain, central Qiangtang, Qinghai—Tibet Plateau, and its significance. Geological Bulletin of China, 26(8): 1003~1008.

Li Xueren, Wang Jian, Cheng Leli, Fu Xiugen, Wang Yuke. 2018. New insights into the Late Triassic Nadigangri Formation of northern Qiangtang, Tibet, China: Constraints from U-Pb ages and Hf isotopes of detrital and magmatic Zircons. Acta Geologica Sinca (English Edition), 92: 1451~1467.

Mattioli E, Pittet B, Petipierre L, Mailliot S. 2009. Dramatic decrease of pelagic carbonate production by nannoplankton across the Early Toarcian anoxic event (T-OAE). Global and Planetary Change, 65: 134~145.

McElwain J C, Wade-Murphy J, Hesselbo S P. 2005. Changes in carbon dioxide during an oceanic anoxic event linked to intrusion into Gondwana coals. Nature, 435: 479~482.

Metcalfe I. 2013. Gondwana dispersion and Asian accretion: Tectonic and palaeogeographic evolution of eastern Tethys. Journal of Asian Earth Sciences, 66: 1~33.

Metodiev L. 2008. The ammonite zones of the Toarcian in Bulgaria——New evidence, subzonation and correlation with the standard zones and subzones in North-Western Europe. Comptes rendus de l´Académie bulgar des Sciencess: sciences mathe matiques et naturelles, 61(1): 87~132.

Miller K G, Kominz M A, Browning J, Wright J D, Mountain G S, Katz M E, Sugarman P J, Cramer B S, Christie-Blick N, Pekar S. 2005. The Phanerozoic record of global sea-level change. Science, 310(5752), 1293~1298.

Mou Shiyong, Xiong Xingguo, Wang Changwei, Wang Min, Chen Ren, Zeng Changxing, Lu Dingbiao, Yue Long, Yi Chengxing, Huo Yongzhong, Zhu Xun, Bian Shenwu, Xu Anquan, Kuang Zhong, Zhao Weili. 2017#. Regional Geological Report (1:25,0000) for Dinggu, P. R. C. Beijing: Geological Publishing House, 55~58.

Pan Guitang, Wang Liquan, Li Rongshe, Yuan Sihua, Ji Wenhua, Zhang Wanping, Wang Baodi. 2012. Tectonic evolution of the Qinghai—Tibet Plateau. Journal of Asian Earth Sciences, 53: 3~14.

Reolid M, Duarte L V, Rita P. 2019. Changes in foraminiferal assemblages and environmental conditions during the T-OAE (Early Jurassic) in the northern Lusitanian Basin, Portugal. Palaeogeography, Palaeoclimatology, Palaeoecology, 520: 30~43.

Röhl H J, Schmid-Röhl A, Oschmann W, Frimmel A, Schwark L. 2001. The Posidonia Shale (Lower Toarcian) of SW-Germany: an oxygen-depleted ecosystem controlled by sea level and palaeoclimate. Palaeogeography, Palaeoclimatology, Palaeoecology, 165: 27~52.

Ruhl M, Veld H, Kürschner W M. 2010. Sedimentary organic matter characterization of the Triassic—Jurassic boundary GSSP at Kuhjoch (Austria). Earth and Planetary Science Letters, 292 (1~2): 17~26.

Sabatino N, Neri R, Bellanca A, Jenkyns H C, Baudin F, Parisi G, Masetti D. 2009. Carbon-isotope records of the Early Jurassic (Toarcian) oceanic anoxic event from theValdorbia (Umbria—Marche Apennines) and Monte Mangart (Julian Alps) sections: palaeoceanographic and stratigraphic implications. Sedimentology 56: 1307~1328.

Seyed-Emami K, Fürsich, F T, Wilmsen M, Majidifard M R, Shekarifard A. 2008. Lower and Middle Jurassic ammonoids of the Shemshak Group in Alborz, Iran and their palaeobiogeographical and biostratigraphical importance. Acta Palaeontologica Polonica, 53 (2): 237~260.

Tan Fuwen, Wang Jian, Li Yongtie, Du Baiwei, Zhu Zhongfa. 2004&. Late Jurassic—Early Cretaceous strata and their sedimentary characteristics in the Qiangtang Basin, northern Tibet. Chinese Geology, 31(4): 400~405.

Tejada M L G, Mahoney J J, Duncan R A, Hawkins M P. 1996. Age and geochemistry of basement and alkalic rocks of Malaita and Santa Isabel, Solomon Islands, southern margin of Ontong Java Plateau. Journal of Petrology, 37: 361~394.

Tribovillard N, Algeo T J, Lyons T, Riboulleau A. 2006. Trace metals as paleoredox and paleoproductivity proxies: an update. Chemical Geology, 232: 12~32.

Wang Jian, Tan Fuwen, Li Yalin, Li Yongtie, Wang Chengshan, Guo Zhujun, Wang Xiaolong, Du Baiwei, Zhu Zhongfa. 2004&. The Potential of the Oil and Gas Resources in Major Sedimentary Basins on the Qinghai—Xizang Plateau. Beijing: Geological Publishing House, 34~88.

Wang Jian, Wang Zhengjian, Chen Wwenxi, Fu Xiugen, Chen Ming. 2007&. New evidences for the age assignment of the Nadi Kangri Formation in the North Qiangtang basin, northern Tibet, China. Geological Bulletin of China, 26(4): 404~409.

Wang Jian, Fu Xiugen, Chen Wenxi, Wang Zhengjian, Tan Fuwen, Chen Ming, Zhuo Jiewen. 2008. Chronology and geochemistry of the volcanic rocks in Woruo mountain region, northern Qiangtang depression: implications to the Late Triassic volcanic—sedimentary events. Science in China series D: Earth Science, 51(2): 194~205.

Wang Jian, Fu Xiugem, Chen Wenxi, Tan Fuwen, Wang Zhengjiang, Chen Ming, Zhuo Jiewen. 2008#. Chronology and geochemistry of the volcanic rocks in Woruo mountain region, northern Qiangtang depression: implications to the Late Triassic volcanic—sedimentary events. Science in China series D: Earth Science, 38 (1): 33~

43.

Wang Jian, Fu Xiugen, Tan Fuwen, Chen Ming, He Jianglin. 2010&. A New Sedimentary Model for the Qiangtang Basin. Acta Sedimentologica Sinica, 28(5): 884~893.

Wang Jian, Fu Xiugen. 2018&. Sedimentary evolution of the Qiangtang Basin. Chinese Geology, 45(2): 237~259.

Wang Xuance, Li Jie. 2013. Re-Os dating of the Shenglihe marine oil shale, North Tibet——A development method for direct dating crude oil. Second annual conference for Key Laboratory for Sedimentary Basin and Oil and Gas Resources: 6.

Wei Hengye, Algeo T J, Yu Hao, Wang Jiangguo, Guo Chuan, Shi Guo. 2015. Episodic euxinia in the Changhsingian (late Permian) of South China: evidence from framboidal pyrite and geochemical data. Sedimentary Geology, 319: 78~97.

Wignall P B, Newton R. 1998. Pyrite framboid diameter as a measure of oxygen deficiency in ancient mudrocks. American Journal of Science 298: 537~552.

Wilkin R T, Arthur M A. 2001. Variations in pyrite texture, sulfur isotope composition, and iron systematics in the Black Sea: Evidence for late Pleistocene to Holocene excursions of the O_2—H_2S redox transition. Geochimica et Cosmochimica Acta, 65: 1399~1416.

Wissler L, Funk H, Weissert H. 2003. Response of Early Cretaceous carbonate platforms to changes in atmospheric carbon dioxide levels. Palaeogeography, Palaeoclimatology, Palaeoecology, 200: 187~205.

Wissler L, Weissert H, Buonocunto F P, Ferreri V, D´Argenio B. 2004. Calibration of the early Cretaceous time scale. Calibration of the Early Cretaceous time scale: a combined chemostratigraphic and cyclostratigraphic approach to the Barremian—Aptian interval Campania Apennines and southern Alps (Italy). In: D´Argenio B, Fischer A G, Premoli-Silva I, Weissert H, Ferreri V. eds. Cyclostratigraphy: Approaches and case histories. Special Publications of SEPM, 81: 123~134.

Yan Maodu, Zhang Dawen, Fang Xiaomin, Ren Haidong, Zhang Weilin, Zan Jinbo, Song Chunhui, Zhang Tao. 2016. Paleomagnetic data bearing on the Mesozoic deformation of the Qiangtang Block: Implications for the evolution of the Paleo-and Meso-Tethys. Gondwana Research, 39: 292~316.

Yi Haisheng, Lin Jinhui, Zhao Bing, Li Yong, Shi He, Zhu Lidong. 2003&. New biostratigraphic data of the Qiangtang area in the northern Tibetan Plateau. Geological Review, 49: 59~65.

Yin Jiarui, Gao Jinhai, Wang Yongsheng, Zhang Shuqi, Zheng Chunzi, Xu Debiao, Bai Zhida, Sun Lixin, Su Xin. 2006&. Jurassic ammonites in anoxic black shales from Sewa and Amdo, northern Tibet. Acta Palaeontologica Sinica, 45: 311~331.

Zhai Qingguo, Li Cai. 2007&. Zircon SHRIMP dating of volcanic rock from the Nadigangri Formation in Juhuashan, Qiangtang, northern Tibet and its geological significance. Acta Geologica Sinica, 81(6): 795~801.

Zhang Xiuzheng, Dong Yongsheng, Wang Qiang, Dan Wwei, Zhang Chunfu, Deng Mingrong, Xu Wang, Xia Xiaoping, Zeng Jipeng, Liang He. 2016. Carboniferous and Permian evolutionary records for the Paleo-Tethys Ocean constrained by newly discovered Xiangtaohu ophiolites from central Qiangtang, central Tibet. Tectonics, 35: doi:10.1002/2016TC004170.

Zhu Tongxing, Feng Xingtao, Lin Shiliang, Zhang Z henggui, Zhou Mingkui. 2012#. Regional Geological Report (1:25,0000) for HeiHuling, P. R. C. Beijing: China University of Geosciences Press, 24~56.

Oceanic anoxic events in the Mesozoic Qiangtang Basin and global comparison

FU Xiugen[1, 2, 3], WANG Jian[1, 2, 3], ZENG Yuhong[1, 2], SONG Chunyan[4], ZENG Shengqiang[4]

1) *Qiangtang Institute of Sedimentary Basin*, *Southwest Petroleum University*, *Chengdu*, 610050;

2) *School of Geoscience and Technology*, *Southwest Petroleum University*, *Chengdu*, 610050;

3) *State Key Laboratory of oil and Gas Reservior Geology and Exploitation* (*Southwest Petroleum University*), *Chengdu*, 610050;

4) *Chengdu Center*, *China Geological Survey*, *Chengdu*, 610081

Abstract: Qiangtang Basin is the largest Jurassic marine basin in China, located in the northern part of the Qinghai—Tibet Plateau, and thus, the Mesozoic marine succession has been well documented in this basin. A series of ocean anoxic events occurred during the sedimentary evolution of the Mesozoic Qiangtang Basin. This paper summarized the major achievements of these ocean anoxic events. The carbonate carbon-isotope record contains two different excursions across the marine T—J transition in the Qiangtang Basin. These are consistent with the "initial" and "main" negative carbon-isotope excursions (CIE) found in the global stratotype section and point (GSSP) of the T—J boundary. The depositional environments change from oxic to anoxic conditions across the T—J boundary. During the early evolution of basin, the carbon-isotope profile exhibits a distinct negative excursion in the Bilong Lake area. This excursion is similar to negative CIE found in GSSP of the Early Toarcian ocean anoxic event, suggesting that the Early Toarcian ocean anoxic event is extensive in the Qiangtang Basin. A large-scale regression occurred during the late evolution of the Qiangtang Basin. In this interval, the sediments only deposited in the Northern Qiangtang Depression consisting shale, oil shale, mudstone, and marl. A high-resolution carbon-

isotope record from these strata revealed a characteristic and well-correlatable Barremian—Lower Aptian pattern. This result is consistent with well-preserved patterns observed in the southern, northern, and northwestern Tethys, suggesting that the Barremian ocean anoxic event was recorded in the Qiangtang Basin.

Keywords: marine T—J boundary (marine J/T boundary); Toarcian ocean anoxic event; Barremian ocean anoxic event; Qiangtang Basin

Acknowledgements: This work was supported by the National Natural Science Foundation of China (No. 91955204) and the second Tibetan Plateau Scientific Expedition and Research Program (STEP) (No. 2019QZKK080301)

First author: FU Xiugen, male, born in 1976, professor, mainly working on sedimentology, petroleum geology, and event geology; Email: fuxiugen@126.com

Manuscript received on: 2020-07-10; Accepted on: 2020-08-20; Edited by: LIU Zhiqiang

Doi: 10.16509/j.georeview.2020.05.004